ACS APPLIED MATERIALS & INTERFACES

Research Article

www.acsami.org

Composite Electronic Materials Based on Poly(3,4-propylenedioxythiophene) and Highly Charged Poly(aryleneethynylene)-Wrapped Carbon Nanotubes for Supercapacitors

Mariem R. Rosario-Canales,[†,‡] Pravas Deria,[§] Michael J. Therien,*[,§] and Jorge J. Santiago-Avilés*[,‡]

[†]Department of Chemistry and [‡]Department of Electrical and Systems Engineering, University of Pennsylvania, Philadelphia, Pennsylvania 19104, United States

[§]Department of Chemistry, French Family Science Center, 124 Science Drive, Duke University, Durham, North Carolina 27708, United States

Supporting Information

ABSTRACT: Supercapacitor charge storage media were fabricated using the semiconducting polymer poly(3,4-propylenedioxythiophene) (PProDOT) and single-walled carbon nanotubes (SWNTs) that were helically wrapped with ionic, conjugated poly[2,6-{1,5-bis(3-propoxysulfonicacidsodiumsalt)}naphthylene]ethynylene (PNES). These PNES-wrapped SWNTs (PNES-SWNTs) enable efficient dispersion of individualized nanotubes in a wide range of organic solvents. PNES-SWNT film-modified Pt electrodes were prepared by drop casting PNES-SWNT suspensions in MeOH; high stability, first-generation PProDOT/PNES/SWNT composites were realized via electropolymerization of the ProDOT parent monomer (3,4-propylenedioxythiophene) in a 1-ethyl-3-methylimidazolium bis(trifluoromethylsulfonyl)imide/propylene carbonate solution at the PNES-SWNT-modified electrode. The electrochemical properties of PProDOT and PProDOT/PNES/SWNT single electrodes and devices were examined using cyclic voltammetric methods. The hybrid composites were found to enhance key supercapacitor figures of merit (charge capacity and capacitance) by approximately a factor of 2 relative to those determined for benchmark Type I devices that exploited a classic PProDOT-based electrode material. The charge/discharge stability of the supercapacitors was probed by repeated rounds of cyclic voltammetric evaluation at a minimum depth of discharge of 73%; these experiments demonstrated that the hybrid PProDOT/PNES/SWNT composites retained ~90% of their initial charge capacity after 21 000 charge/discharge cycles, contrasting analogous data obtained for PProDOT-based devices, which showed only 84% retention of their initial charge capacity.

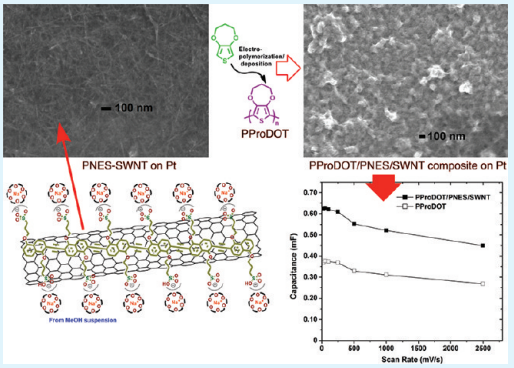

KEYWORDS: *supercapacitor, single-walled carbon nanotubes, semi-conducting polymercharge capacity*

INTRODUCTION

Among the various types of energy storage devices, electrochemical capacitors (ECs, also known as supercapacitors or ultracapacitors) have gathered increasing attention for applications that demand high operating power levels. ECs are envisioned as a technology platform to bridge the gap between conventional capacitors and batteries, which provide, respectively, exceptional power and energy densities. Thus far, applications where ECs are being exploited include hybrid electric vehicles and consumer electronic products.[1,2] There are two general types of supercapacitors, electrochemical double-layer capacitors (EDLCs) and redox capacitors; these devices differ with respect to the manner in which charge is fundamentally stored,[3] and materials for each class have been recently reviewed by Simon and Gogotsi.[4] EDLCs operate based on the charge separation that occurs in the electrical double-layer established at the electrolyte/electrode interface where the electrode is typically a high-specific-surface-area carbonaceous material[5] based on either activated carbon,[6−10] carbon nanotubes (CNTs),[11−18] graphene,[18−24] carbide-derived carbon,[25] or carbon aerogels.[26] In contrast, redox capacitors (pseudocapacitors) do not store charge electrostatically but by Faradaic charge transfer that takes place in the active material, typically a metal oxide (e.g., RuO_2 or MnO_2)[8,10,12,27−31] or an electrically active polymer (EAP).[22,32−39]

Factors that underscore the attractiveness of EAPs as supercapacitor electrode materials include: (i) significantly

Received: August 4, 2011
Accepted: December 2, 2011
Published: December 2, 2011

Chart 1. (A) PNES Structure; (B) Depiction of PNES-SWNTs; and (C) PProDOT Structure

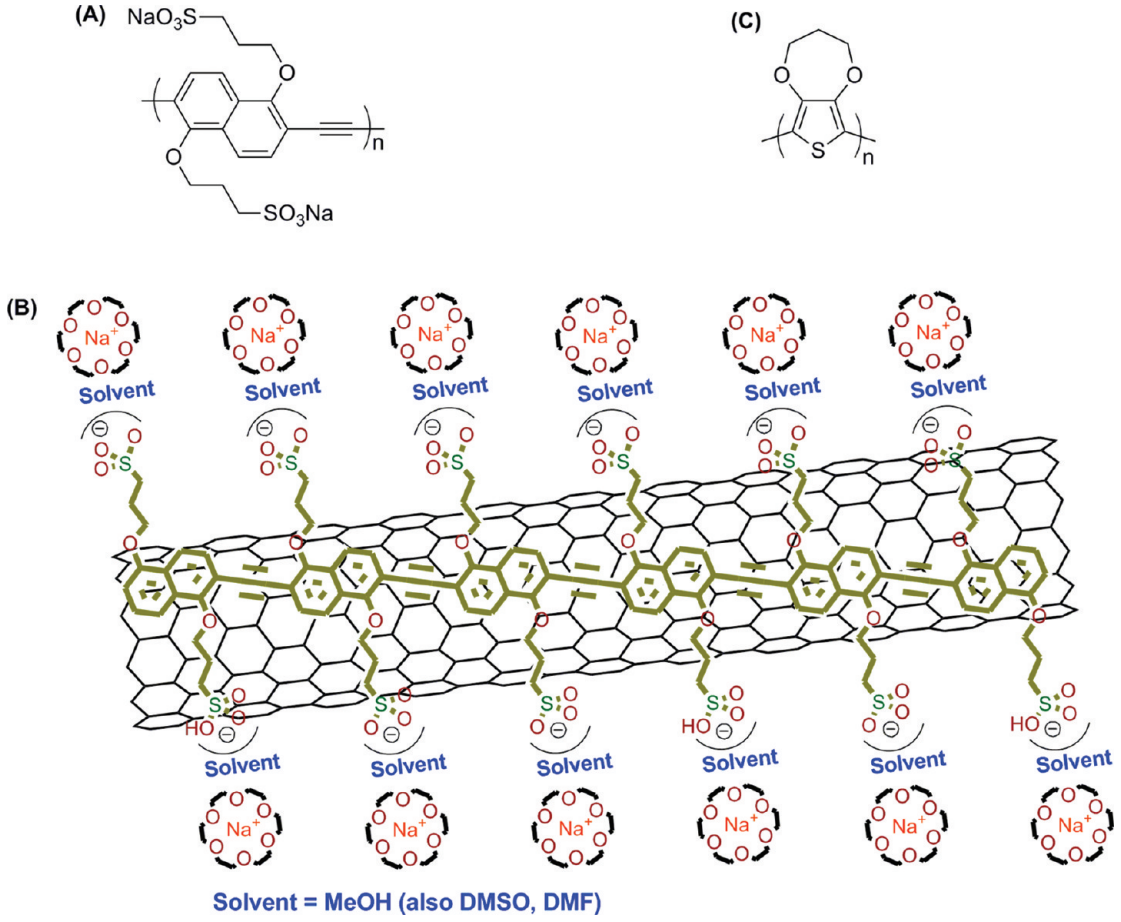

diminished production costs relative to noble metal oxides, (ii) fast charge/discharge kinetics, (iii) the possibility to store charge throughout the entire volume of the material, and (iv) the ability to tailor properties such as conductivity, the operating voltage window, and fundamental charge doping characteristics through chemical modification.[3,35,38] There are at least four types of EAP-based supercapacitors, which are classified by the doping state and combination of materials chosen for electrode construction.[33,35] In Type I supercapacitors, the same p-dopable material is used for both electrodes and the overall cell voltage is generally limited to less than 1 V. Type II supercapacitors feature different p-dopable polymers on each electrode; such systems have demonstrated overall cell voltages up to 1.25 V. Higher energy densities can be achieved with Type III and Type IV supercapacitor configurations. In Type III systems, a polymer capable of being both p- and n-doped is used for electrode construction, while Type IV assemblies exploit disparate n- and p-dopable polymers at the respective electrodes. Some of the most studied EAPs for supercapacitors include polyaniline (PANI),[34] polypyrrole (PPY),[38] polythiophene,[39] and polythiophene derivatives[32,38] such as poly(3,4-ethylenedioxythiophene) (PEDOT).[36,37]

Over the past few years, substantial attention has been focused on the preparation of EAP-CNT composite systems for supercapacitor materials, in an attempt to overcome some of the drawbacks common to EAPs.[40−42] For example, it has been established that redox cycling of polymer-based supercapacitors subjects these materials to repeated rounds of swelling and shrinkage driven by the respective insertion and deinsertion of counterions; these volume changes cause mechanical stresses that contribute to the diminished cycleability of these materials relative to that established for EDLCs.[1,41,42] Combining pseudocapacitive polymeric materials with double-layer capacitive single-walled or multiwalled carbon nanotubes (SWNTs or MWNTs) partially alleviates this problem, likely through: (i) storing a portion of the total charge as a double-layer capacitance in the nanostructures, (ii) enhancing the conductivity of the polymeric active layers in their less conductive dedoped state therefore improving the frequency response, and (iii) providing superior mechanical strength.[41−43]

Several methods for the preparation of EAP/CNT composites have been reported, and their utility as supercapacitor electrode materials demonstrated.[41−52] The most common preparative route involves oxidative chemical polymerization, where the monomer, oxidant, and CNTs are all present in the same reaction medium.[41,42,44−48] This method requires typically the use of a binder for electrode construction. A second approach involves oxidative electrochemical polymerization of the EAP monomer (either potentiostatically or galvanostatically) via (i) initial preparation of a CNT electrode substrate followed by electrodeposition of a semiconducting polymer,[50,51] or (ii) dissolution of an EAP monomeric precursor in a CNT suspension, followed by electrochemical codeposition of the composite onto an electrode surface.[43,49,52] In these electrode materials, PANI- and PPY-based composites are most heavily utilized, as aniline and pyrrole monomers are readily soluble in water; in contrast, superior EAPs such as

EDOT and related thiophene-based polymers, have limited aqueous solubility. For this reason, many approaches to EAP/CNT composites require the use of chemically treated or functionalized CNTs for dispersion in an organic solvent reaction medium.[43,47−49,52] In this regard, it is important to underscore that covalent modification of nanotubes negatively impacts intrinsic CNT semiconducting and conducting properties and therefore supercapacitor performance; additionally, as the electrochemical codeposition approach utilizes no supporting electrolyte, such functionalized CNTs have diminished utility as dopants or charge-balancing counterions during the polymerization process.[43,49,52]

In this study, we exploit noncovalently modified SWNTs in which an aryleneethynylene polymer monolayer helically wraps the nanotube surface at periodic and constant morphology.[53,54] Previous work highlights that ionic poly[2,6-{1,5-bis(3-propoxysulfonicacidsodiumsalt)}naphthylene]ethynylene (PNES) exfoliates and individualizes SWNTs in water and organic solvents such as DMSO, DMF, and MeOH via single chain wrapping; AFM and TEM data demonstrate that **PNES-SWNTs** manifest a helix pitch length =10 ± 2 nm, regardless of solvent.[54] We show herein that the organic solvent solubility of **PNES-SWNTs** enables facile fabrication of EAP/CNT composites and the delineation of novel hybrid supercapacitor materials. Furthermore, we prepare a poly(3,4-propylenedioxythiophene) (PProDOT)-containing **PNES-SWNT** hybrid composite (**PProDOT/PNES/SWNT**) and evaluate its capacitive performance against benchmark PProDOT-based Type I supercapacitor devices, where identical p-dopable materials are utilized for both electrodes. PProDOT was chosen as the EAP for a number of reasons. Besides being easily deposited onto electrode substrates via electropolymerization of the parent monomer in supporting electrolyte solution,[37] PProDOT, a 3,4-alkylenedioxythiophene polymer, possesses both a low oxidation potential and attractive potentiometric switching properties.[37,55,56] The utility of PProDOT in Type I supercapacitors has been demonstrated by Stenger-Smith and co-workers,[37,57] who have shown that improved switching speeds and lifetimes exceeding 50 000 cycles with 98% retention of initial charge capacity can be realized for PProDOT electrodes when using ionic liquid as supporting electrolyte,[37] which make possible low-temperature performance of these devices.[57]

RESULTS AND DISCUSSION

PNES, used in combination with a suitable phase transfer agent, provides individualized, noncovalently modified SWNTs (**PNES-SWNTs**, Chart 1B) of fixed morphology that retain established nanotube semiconducting and conducting properties, in a wide range of dielectric media.[54] High resolution transmission electron microscopy (TEM) (Figure 1) experiments that examine **PNES-SWNT** structures formed in CH_3OH solvent reveal that the **PNES-SWNT** samples used in these experiments are composed overwhelmingly of individualized nanotubes, in which a PNES monolayer helically wraps the nanotube surface with periodic and constant morphology (helix pitch length =10 ± 2 nm), similar to that described previously; such monolayer wrapping minimizes the polymer:SWNT molar ratio of the organic-solvent soluble SWNT composition.[54] In this work, we utilize these semiconducting polymer wrapped SWNT structures as a new component for the evolution of superior supercapacitor electrode materials. The EAP PProDOT (Chart 1c) was

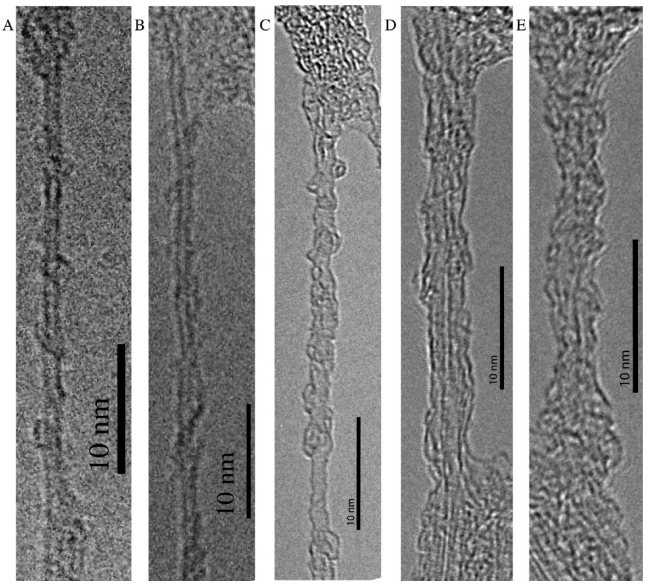

Figure 1. HRTEM images of PNES-wrapped SWNTs obtained from a MeOH suspension: (A−C) individualized tubes, (D, E) small-tube bundles (see the Supporting Information for preparative details).

utilized as the other key constituent for hybrid composite electrode materials incorporating SWNTs. The ionic liquid (IL), 1-ethyl-3-methylimidazolium bistrifluoromethanesulfonimidate (EMIBTI), dissolved in anhydrous propylene carbonate (PC), was chosen as the electrolyte solution for both the preparation and evaluation of first-generation **PProDOT/PNES/SWNT** composites and benchmark PProDOT electrode materials, as imidazolium electrolytes possess excellent electrochemical and thermal stability, good conductivity, and serve to maximize switching speed.[37,58]

Of the approaches discussed previously for the preparation of EAP/CNT composites for supercapacitors, electrochemical polymerization on CNT-modified surfaces was chosen as the initial route to obtain such materials. Thus, electropolymerization of ProDOT (18.6 mM) in a 0.077 M EMIBTI/PC electrolyte solution at a Pt button electrode was used to generate the PProDOT electrode material, while PProDOT electrodeposition under the same conditions at a **PNES-SWNT** film-modified Pt electrode provided the hybrid composite material. Figure S1 in the Supporting Information shows the respective multisweep voltammograms for the electropolymerization at Pt and **PNES-SWNT**-modified Pt surfaces (scan rate (ν) = 100 mV/s)). Note that a trace crossing on the reverse scan occurred during the first cycle for the electropolymerization of ProDOT at Pt surfaces (see Figure S1 in the Supporting Information); this phenomenon has been identified previously as a nucleation loop that signifies the growth of a conducting polymer film on freshly polished electrode surface.[59,60] A single anodic redox process was observed during the first anodic scan corresponding to irreversible oxidation of the ProDOT monomer to its cation radical; the onset potential for monomer oxidation ($E_{m,onset}$) corresponded to +0.95 V vs Fc/Fc^+. The cathodic waves evident on the reverse scan correspond to the reduction of the polymer being deposited at the electrode surface. In contrast to the redox processes observed during electrodeposition at Pt, the electropolymerization of ProDOT at the **PNES-SWNT** film-modified Pt surface proceeded without an initial reverse potentiometric scan nucleation loop (see Figure S1 in the Supporting Information), suggesting some

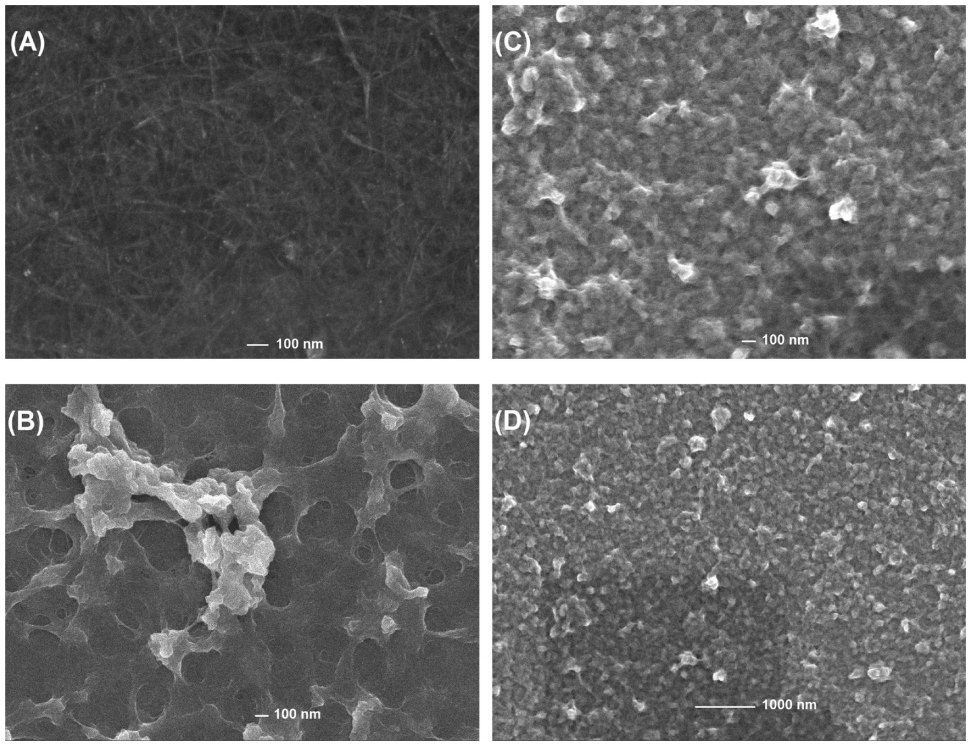

Figure 2. Scanning electron microscopic images of: (A) a **PNES-SWNT** deposited thin film on Pt, (B) and PProDOT eletropolymerized thin film on bare Pt, and (C, D) **PNES-SWNT** modified Pt surfaces. These samples were prepared using conditions identical to that used to produce the supercapacitor electrode materials, save that Pt-coated silicon wafers, instead of Pt button electrodes, were employed as surfaces (see text).

mechanistic disparity for nucleation and growth of the PProDOT film at the **PNES-SWNT**-modified electrode relative to that at the bare noble metal. Also noteworthy is the fact that $E_{m,onset}$ for ProDOT electropolymerization at the **PNES-SWNT** film-modified electrode occurred at a lower potential (+0.57 V vs Fc/Fc^+) relative to that at bare Pt. It is evident from the data in Figure S1 in the Supporting Information that anodic and cathodic peak currents increase with successive potentiometric cycling at both types of electrodes, signaling growth of an electroactive polymer film.

Microscopic characterization of **PNES-SWNT**-modified Pt surfaces, as well as analogous PProDOT and **PProDOT/PNES/SWNT** composites, was carried out on Pt-coated silicon wafers using deposition and electropolymerization methods identical to that described above. Scanning electron microscopy (SEM) experiments that examine a **PNES-SWNT** modified Pt surface (Figure 2A) reveal a highly homogeneous surface coverage of individualized SWNTs, achieved via simple drop casting of a **PNES-SWNT** suspension in methanol. SEM images of PProDOT at bare (Figure 2B) and **PNES-SWNT**-modified Pt surfaces (Figure 2C,D) show uniform, smooth coverage of these electropolymerized materials. AFM images of PProDOT at bare and **PNES-SWNT**-modified Pt surfaces (Figure 3 and Figure S5 in the Supporting Information) corroborate these SEM data.

The charge capacities ($Q_{1/2}$) of the electrosynthesized PProDOT films were measured by integrating the area under the curve of the corresponding current (i) vs time (t) plot for the final deposition cycle. Although $Q_{1/2}$ for the PProDOT film electrodeposited at the Pt surface was 1.160 mC, $Q_{1/2}$ values for the composite materials ranged between 1.904 and 2.312 mC, indicating a 1.5-to-2-fold increase in the charge capacity of these first-generation hybrid composite materials relative to that for the classic PProDOT benchmark. Note that PProDOT films electrosynthesized at Pt surfaces were purple in appearance, whereas the composites formed via PProDOT electrodeposition at **PNES-SWNT** film-modified electrodes were blackish purple. It is also worth noting that **PProDOT/PNES/SWNT** composite films showed better adherence to the Pt current collectors in comparison to homogeneous PProDOT compositions; film peeling and surface degradation of PProDOT at Pt were evident over time, suggesting improved mechanical robustness of the **PProDOT/PNES/SWNT** composites.[61]

Following electropolymerization, the resulting PProDOT benchmark and composite films were rinsed with monomer-free electrolyte solution, and cyclic voltammetric responses were recorded at scan rates ranging between 25 and 250 mV/s over a −1.5 to +0.4 V potential window. Figure 4 shows the cyclic voltammetric responses recorded at ν = 100 mV/s for the pure polymer film and the hybrid composite. Two oxidation and two reduction peaks were distinguished in both cases; with increasing scan rate, the cathodic peak potentials (E_{pc} values) shift negatively and the anodic peak potential (E_{pa} value) shift positively, as expected. Plots of the peak current versus ν (see Figure S2 in the Supporting Information) are linear, indicating that the polymer film is electrode supported and electroactive. The Figure 4 data depict fast current switching at the terminal anodic potential congruent with capacitive behavior, contrasting the $i-V$ behavior observed at the cathodic switching potential, where the currents taper, indicative of reduction or dedoping of the polymer to its neutral insulating state. The Figure 4 voltammograms, however, highlight important differences between pristine PProDOT and **PProDOT/PNES/SWNT** composite films. Note that the **PProDOT/PNES/SWNT** composite shows an output current enhancement more

dx.doi.org/10.1021/am201041p | *ACS Appl. Mater. Interfaces* 2012, 4, 102−109

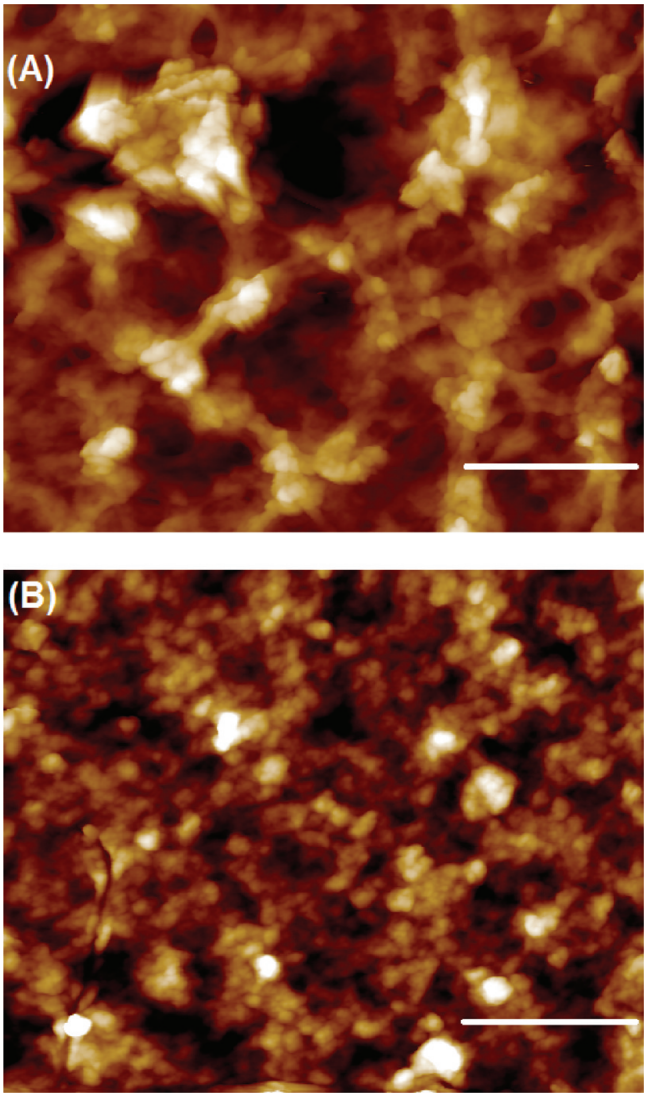

Figure 3. Topographic intermittent contact mode AFM images of: (A) a PProDOT eletropolymerized thin film on bare Pt, and (B) a **PNES-SWNT**-modified Pt surface. These samples were prepared using conditions identical to that used to produce the supercapacitor electrode materials, save that platinum-coated silicon wafers, instead of Pt button electrodes, were employed as surfaces (see text).

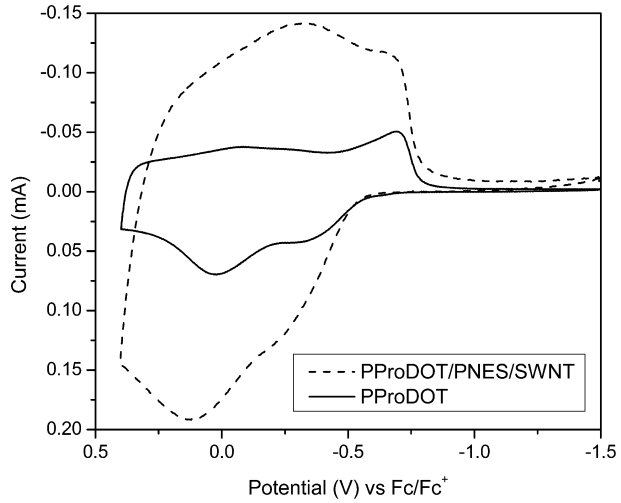

Figure 4. Cyclic voltammetric responses recorded at a scan rate of 100 mV/s of single electrode films composed of PProDOT and **PProDOT/PNES/SWNT** composite materials evaluated in monomer-free electrolyte solution (0.077 M EMIBTI/PC).

Scheme 1. Schematic of the Prototype Supercapacitor Devices, Based on a Modified[62] Literature Design,[63] That Were Utilized in This Study

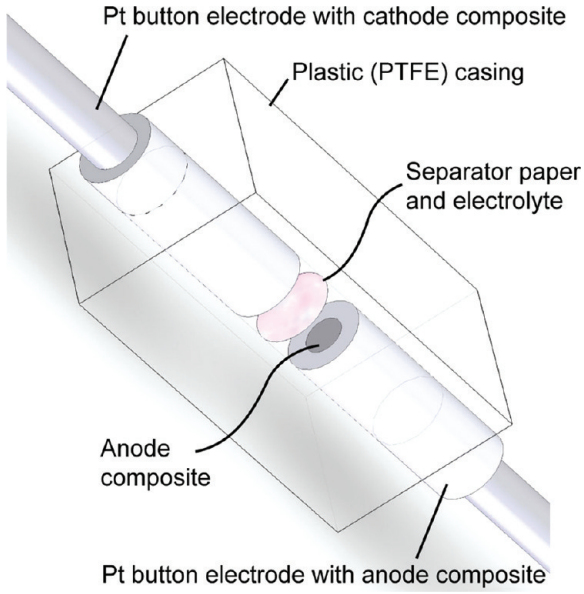

than a factor of 2 larger than that observed for the corresponding PProDOT film, underscoring its enhanced capacitive properties. Furthermore, the larger magnitude current observed at the negative end of the voltammogram of the **PProDOT/PNES/SWNT** composite relative to that for the PProDOT film strongly suggests improved conductivity of the hybrid material; it should be noted, however, that SWNT-derived double layer and redox capacitances play roles in this observed enhanced charge storage capacity as well, though these contributions are generally thought to be small relative to the overall pseudocapacitance of the polymer.

Benchmark prototype supercapacitor devices were assembled using PProDOT- and **PProDOT/PNES/SWNT**-based electrodes and probed in a standard 2-electrode configuration (Scheme 1) that exploited a modified[62] literature design.[63] As assembled, one film (composite) in these devices resides in its p-doped or oxidized state, while the other film (composite) is maintained in its neutral state - this represents the initial charged state of the supercapacitor. For the PProDOT-based supercapacitors, the oxidized PProDOT film on the Pt surface manifested a clear light blue-purple appearance, while the corresponding oxidized **PProDOT/PNES/SWNT** composite-modified Pt electrode appeared emerald green. The neutral films on both the Pt and **PNES-SWNT** film-modified Pt electrode surfaces were purple. Following device assembly, the dependence of $Q_{1/2}$ upon scan rate (25 mV/s < ν < 5000 mV/s) was analyzed up to an upper 0.5 V limit. The cyclic voltammetric responses obtained for the pure polymer and hybrid composite-based devices as a function of scan rate are shown in Figure S3 in the Supporting Information. Note that while both PProDOT- and **PProDOT/PNES/SWNT**-based devices show a fast switching response, as evidenced by the rectangular-shaped voltammograms associated with ideal capacitor behavior, the composite-based device best approx-

imates the behavior of an ideal capacitor. The almost vertical, large magnitude current displacements observed at the cathodic (0.0 V) and anodic (0.5 V) switching potentials for these supercapacitor devices are indicative of negligible interfacial and contact resistance. While rectangular-shaped CVs were also obtained at a 2500 mV/s scan rate, scan rates that approached 5000 mV/s for these supercapacitors displayed deviations from the rectangular behavior highlighted in the data in Figure S3 in the Supporting Information (data not shown); for example, the measured $Q_{1/2}$ value at ν = 5000 mV/s was ~60% of the respective values determined at 25 mV/s for the PProDOT- and **PProDOT/PNES/SWNT**-based devices.

Figure 5A displays the scan rate dependence (25 mV/s < ν < 5000 mV/s) of $Q_{1/2}$ determined for PProDOT- and

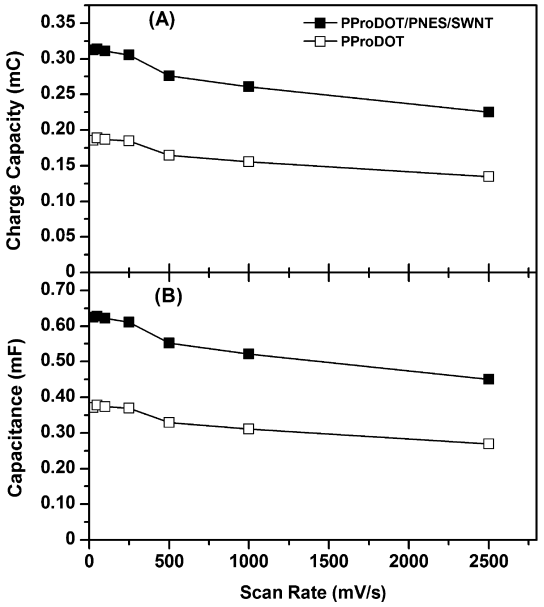

Figure 5. Scan rate dependence of (A) the charge capacity and (B) the capacitance for PProDOT- and **PProDOT/PNES/SWNT**-based supercapacitors.

PProDOT/PNES/SWNT-based supercapcitors. At scan rates ≤250 mV/s, $Q_{1/2}$ was observed to be essentially independent of ν for both film- and composite-based devices, while a 25% drop of the maximum capacity realized occurred when cycling between the cathodic (0.0 V) and anodic (0.5 V) switching potentials at rates faster than 2500 mV/s. Figure 5A also shows that the maximum $Q_{1/2}$ for the PProDOT-based devices peaks at 0.189 mC, contrasting the analogous 0.314 mC value measured for the **PProDOT/PNES/SWNT** composites, highlighting that these first generation hybrid materials manifest ~1.6 fold greater charge capacity relative to PProDOT benchmark films. Coulombic efficiencies, calculated from the integrated cathodic-to-anodic charge ratio, exceeded 96% for all scan rates evaluated (25 mV/s < ν < 5000 mV/s) for both the pure polymer and hybrid composite devices. Figure 5B highlights the dependence of the measured value of the capacitance (C) as a function of ν, calculated using the equation

$$C = Q_{1/2}/V_d \quad (1)$$

where V_d is the device voltage. As expected, the hybrid supercapacitor prototypes based on the **PProDOT/PNES/SWNT** composites featured higher capacitances relative to benchmark Type I devices that exploited PProDOT. The greatest C attained with the pure polymer device was 0.377 mF, significantly less than the 0.627 mF maximum capacitance obtained for the composite device. C was also calculated by normalizing the average current (i_{avg}) relative to ν; these values were similar to those obtained using eq 1. The higher measured values of C for the **PProDOT/PNES/SWNT**-based hybrid devices can be attributed at least in part to the presence of the PNES-wrapped SWNT constituent, which augments the PProDOT redox capacitance with a capacitive double-layer charge-storage contribution. Future work aims to delineate the extent to which each capacitive mechanism contributes to overall charge storage in **PProDOT/PNES/SWNT**-based supercapacitors, and determine whether **PNES-SWNTs** contribute significantly to the pseudocapacitance of these hybrid materials through a PProDOT-independent Faradaic charge transfer process.

Volume changes associated with the cyclical, charge/discharge-coupled insertion/deinsertion of counterions in EAP-based supercapcitors cause mechanical stresses in these polymer films that limit their charge storage utility relative to EDLCs. In this regard, repetitive CV scanning experiments that probe the charge/discharge stability of these active electrode materials underscore added benefits of **PProDOT/PNES/SWNT**-based supercapacitors. Figure S4 in the Supporting Information shows cyclic voltammetric 1000-cycle-life tests (ν = 2500 mV/s; cathodic switching potential = 0.0 V; anodic switching potential = 0.5 V) for both PProDOT- and **PProDOT/PNES/SWNT**-based supercapacitors. At this particular ν, the depth of discharge (DOD) was 73% for both supercapacitors. After completion of these tests, an analysis of charge capacity retention was performed by cycling at 250 mV/s, where the maximum charge-storage capacity was originally determined. The pure polymer-based devices evinced 89% retention of the maximum charge capacity, while the corresponding devices fabricated from **PProDOT/PNES/SWNT** composites featured 92% retention. Following the initial 1000 cycles, these devices were subject to an additional 20 000 charge−discharge cycles (for a total of 21 000 cycles) under the experimental conditions described above. Following a similar analysis, it was demonstrated that the PProDOT benchmark supercapacitor exhibited a 16% loss in maximum charge-storage capacity, relative to only an 11% measured in the composite-based supercapacitors, congruent with the expectation that the **PNES-SWNT** network helps stabilize PProDOT against mechanical stress associated with the cyclical insertion/deinsertion of counterions that occurs with continual rounds of device charging and discharge.

In conclusion, supercapacitor charge storage media were fabricated using the semiconducting polymer poly(3,4-propylenedioxythiophene) (PProDOT) and single-walled carbon nanotubes (SWNTs) that were helically wrapped with ionic, conjugated poly[2,6-{1,5-bis(3-propoxysulfonicacidsodiumsalt)}naphthylene]ethynylene (PNES). These composites were prepared by electrochemical polymerization of the ProDOT parent monomer in a 1-ethyl-3-methylimidazolium bis(trifluoromethylsulfonyl)imide/anhydrous propylene carbonate supporting electrolyte solution at a **PNES-SWNT**[64]-modified Pt electrode surface. Hybrid **PProDOT/PNES/SWNT** materials were found to enhance supercapacitor charge storage and capacitance figures of merit by nearly a factor of 2 of relative to corresponding supercapacitors fabricated using only pristine PProDOT.

These **PProDOT/PNES/SWNT**-based supercapacitors furthermore retain 90% of their initial maximum charge capacity after 21 000 charge/discharge cycles, exhibiting superior durability and performance relative to analogous PProDOT-derived benchmark devices. Such high level charge−discharge cycling stability lacks precedent in previously established organic supercapacitor materials. These results underscore the potential of **PNES-SWNT** compositions in supercapacitor applications, and suggest that new types of organic semiconductor/SWNT composites may enable simultaneous enhancement of charge capacity, capacitance, charge mobility, and mechanical stability in organic charge-storage media that exploit high surface area nanoscale carbon.

METHODS

A detailed description of materials and experimental methods are provided in the Supporting Information.

PProDOT/PNES/SWNT Supercapacitor Composites. The synthesis and extensive characterization of **PNES-SWNTs** have been reported previously.[54] **PNES-SWNT** suspensions in MEOH solvent were prepared similarly to those described in a previously reported procedure.[54] In brief, PNES (1.64 mg/mL; $M_n \approx 18.8$ kD; DP ≈ 40; PDI ≈ 1.11) was dissolved in MeOH solvent with the phase transfer catalyst 18-crown-6 (~21 mg/mL). This solution (2.5 mL) was direct-tip sonicated (1 h; 1.2 W/mL; 20 kHz) with 3.1 mg of HipCo SWNTs (purified; lot P0343), and centrifuged (@~45 000 g; 1:30 h); further details are provided in the Supporting Information. PProDOT was electrochemically synthesized at bare Pt and **PNES-SWNT** film-modified Pt electrodes (0.2 cm^2) under nitrogen. Polymer deposition was achieved via a standard cyclic voltammetric method in a single-compartment, three-electrode cell (experimental conditions: respective cathodic and anodic switching potentials, −1.5 and +1.1 V; scan rate (ν) = 100 mV/s; potentiometric cycles = 24). **PNES-SWNT** film-modification of the Pt electrode, prior to PProDOT deposition, involved successive drop casting of **PNES-SWNT** suspensions in MeOH solvent (8 μL), followed by drying under vacuum. Following electrochemical deposition of the electrically active PProDOT, the charge capacities ($Q_{1/2}$) of the films were measured by integrating the area under the current (i) vs time (t) curve obtained for the last deposition cycle. Cyclic voltammetric responses of the PProDOT and **PProDOT/PNES/SWNT** composite films were analyzed in a monomer-free electrolyte solution [1-ethyl-3-methylimidazolium bistrifluoromethanesulfonimidate/anhydrous propylene carbonate (EMIBTI/PC)] over a series of scan rates between 25 and 250 mV/s. Supercapacitor assembly and evaluation were carried out at room temperature under a nitrogen atmosphere. The electrode materials in all devices consisted of one p-doped PProDOT- and one neutral PProDOT-based film; both films were rinsed with monomer-free electrolyte solution prior to assembling the device. PProDOT benchmark redox devices were assembled with the two PProDOT-based electrodes in a vertical, cofacial configuration; these modified electrodes were fitted snuggly inside an ultrahigh-molecular-weight (UHMW) polyethylene casing. Similar electrochemical cells were assembled using the hybrid **PProDOT/PNES/SWNT**-modified electrodes. One sheet of porous separator paper (90 μm thick) wetted with 0.077 M EMIBTI/PC electrolyte was placed between the electrodes. Evaluation of these cells at different potential limits and scan rates was accomplished via two-electrode cyclic voltammetry using the Pine AFCBP1 Bipotentiostat, with the reference and auxiliary electrodes shorted together. Device cycle life tests were carried out via repetitive cyclic voltammetry; in these evaluations, the devices were allowed to equilibrate for 10 s before ramping the voltage to the appropriate potential limits.

ASSOCIATED CONTENT

Supporting Information

PNES-SWNT preparative procedures, ProDOT electropolymerization protocols, electrochemical data, details regarding device assembly, and supercapacitor evaluation.This material is available free of charge via the Internet at http://pubs.acs.org.

AUTHOR INFORMATION

Corresponding Author

*Tel: 919-660-1670 (M.J.T.); 215-898-5167 (J.J.S.-A.). Fax: 919-660-1605 (M.J.T.); 215-573-2068 (J.J.S.-A.). michael.therien@duke.edu (M.J.T.); santiago@seas.upenn.edu (J.J.S.-A.).

ACKNOWLEDGMENTS

This work was supported by a grant from the Office of Naval Research N00014-06-1-0360 and the Nano/Bio Interface Center through the National Science Foundation NSEC DMR-045780. The authors are grateful to Dr. Douglas Yates of the Penn Regional Nanotechnology Facility for assistance with the TEM studies, Dr. Samia Zrig for NMR characterization, and Dr. John Stenger-Smith from NAWCWD, China Lake, for the many insightful discussions.

REFERENCES

(1) Kötz, R.; Carlen, M. *Electrochim. Acta* **2000**, *45*, 2483−2498.
(2) Miller, J. R.; Burke, A. F. *Electrochem. Soc. Interface* **2008**, *17*, 53−55.
(3) Conway, B. E. *Electrochemical Supercapacitors: Scientific Fundamentals and Technological Applications*; Kluwer Academic/Plenum Publishing: New York, 1999.
(4) Simon, P.; Gogotsi, Y. *Nat. Mater.* **2008**, *7*, 845−854.
(5) Zhang, L. L.; Zhao, X. S. *Chem. Soc. Rev.* **2009**, *38*, 2520−2531.
(6) Gamby, J.; Taberna, P. L.; Simon, P.; Fauvarque, J. F.; Chesneau, M. *J. Power Sources* **2001**, *101*, 109−116.
(7) Raymundo-Piñero, E.; Kierzek, K.; Machnikowski, J.; Béguin, F. *Carbon* **2006**, *44*, 2498−2507.
(8) Gao, P.-C.; Lu, A.-H.; Li, W.-C. *J. Power Sources* **2011**, *196*, 4095−4101.
(9) Wen, Z.; Liu, Y.; Liu, A.; Zhu, T.; Zheng, X.; Gao, Q.; Wang, D.; Hu, Z. *Funct. Mater. Lett.* **2010**, *3*, 201−205.
(10) Wang, H.-Q.; Li, Z.-S.; Huang, Y.-G.; Li, Q.-Y.; Wang, X.-Y. *J. Mater. Chem.* **2010**, *20*, 3883−3889.
(11) Izadi-Najafabadi, A.; Futaba, D. N.; Iijima, S.; Hata, K. *J. Am. Chem. Soc.* **2010**, *132*, 18017−18019.
(12) Hou, Y.; Cheng, Y.; Hobson, T.; Liu, J. *Nano Lett.* **2010**, *10*, 2727−2733.
(13) Zhou, R.; Meng, C.; Zhu, F.; Li, Q.; Liu, C.; Fan, S.; Jiang, K. *Nanotechnology* **2010**, *21*, 345701.
(14) Futaba, D. N.; Hata, K.; Yamada, T.; Hiraoka, T.; Hayamizu, Y.; Kakudate, Y.; Tanaike, O.; Hatori, H.; Yumura, M.; Iijima, S. *Nat. Mater.* **2006**, *5*, 987−994.
(15) Picó, F.; Rojo, J. M.; Sanjuán, M. L.; Ansón, A.; Benito, A. M.; Callejas, M. A.; Maser, W. K.; Martínez, M. T. *J. Electrochem. Soc.* **2004**, *151*, A831−A837.
(16) Shiraishi, S.; Kurihara, H.; Okabe, K.; Hulicova, D.; Oya, A. *Electrochem. Commun.* **2002**, *4*, 593−598.
(17) Izadi-Najafabadi, A.; Yamada, T.; Futaba, D. N.; Hatori, H.; Iijima, S.; Hata, K. *Electrochem. Commun.* **2010**, *12*, 1678−1681.
(18) Yang, S.-Y.; Chang, K.-H.; Tien, H.-W.; Lee, Y.-F.; Li, S.-M.; Wang, Y.-S.; Wang, J.-Y.; Ma, C.-C. M.; Hu, C.-C. *J. Mater. Chem.* **2011**, *21*, 2374−2380.
(19) Liu, C.; Yu, Z.; Neff, D.; Zhamu, A.; Jang, B. Z. *Nano Lett.* **2010**, *10*, 4863−4868.
(20) Wang, Y.; Shi, Z.; Huang, Y.; Ma, Y.; Wang, C.; Chen, M.; Chen, Y. *J. Phys. Chem. C* **2009**, *113*, 13103−13107.

(21) Stoller, M. D.; Park, S.; Zhu, Y.; An, J.; Ruoff, R. S. *Nano Lett.* **2008**, *8*, 3498−3502.
(22) Wang, H.; Hao, Q.; Yang, X.; Lu, L.; Wang, X. *Electrochem. Commun.* **2009**, *11*, 1158−1161.
(23) Gómez, H.; Ram, M. K.; Alvi, F.; Villalba, P.; Stefanakos, E.; Kumar, A. *J. Power Sources* **2011**, *196*, 4102−4108.
(24) Kim, T. Y.; Lee, H. W.; Stoller, M.; Dreyer, D. R.; Bielawski, C. W.; Ruoff, R. S.; Suh, K. S. *ACS Nano* **2011**, *5*, 436−442.
(25) Chmiola, J.; Yushin, G.; Gogotsi, Y.; Portet, C.; Simon, P.; Taberna, P. L. *Science* **2006**, *313*, 1760−1763.
(26) Saliger, R.; Fischer, U.; Herta, C.; Fricke, J. *J. Non-Cryst. Solids* **1998**, *225*, 81−85.
(27) Dong, X.; Shen, W.; Gu, J.; Xiong, L.; Zhu, Y.; Li, H.; Shi, J. *J. Phys. Chem. B* **2006**, *110*, 6015−6019.
(28) Hu, C.-C.; Chang, K.-H.; Lin, M.-C.; Wu, Y.-T. *Nano Lett.* **2006**, *6*, 2690−2695.
(29) Toupin, M.; Brousse, T.; Bélanger, D. *Chem. Mater.* **2004**, *16*, 3184−3190.
(30) Zheng, J. P.; Cygan, P. J.; Jow, T. R. *J. Electrochem. Soc.* **1995**, *142*, 2699−2703.
(31) Ye, J.-S.; Cui, H. F.; Liu, X.; Lim, T. M.; Zhang, W.-D.; Sheu, F.-S. *Small* **2005**, *1*, 560−565.
(32) Fonseca, C. P.; Benedetti, J. E.; Neves, S. *J. Power Sources* **2006**, *158*, 789−794.
(33) Irvin, J. A.; Irvin, D. J.; Stenger-Smith, J. D. In *Handbook of Conducting Polymers*, 3rd ed.; Skotheim, T. A., Reynolds, J., Eds.; Taylor & Francis Group: Boca Raton, FL, 2006, p 9−1.
(34) Bélanger, D.; Ren, X.; Davey, J.; Uribe, F.; Gottesfeld, S. *J. Electrochem. Soc.* **2000**, *147*, 2923−2929.
(35) Rudge, A.; Davey, J.; Raistrick, I.; Gottesfeld, S.; Ferraris, J. P. *J. Power Sources* **1994**, *47*, 89−107.
(36) Ryu, K. S.; Lee, Y.-G.; Hong, Y.-S.; Park, Y. J.; Wu, X.; Kim, K. M.; Kang, M. G.; Park, N.-G.; Chang, S. H. *Electrochim. Acta* **2004**, *50*, 843−847.
(37) Stenger-Smith, J. D.; Webber, C. K.; Anderson, N.; Chafin, A. P.; Zong, K.; Reynolds, J. R. *J. Electrochem. Soc.* **2002**, *149*, A973−A977.
(38) Arbizzani, C.; Mastragostino, M.; Meneghello, L. *Electrochim. Acta* **1996**, *41*, 21−26.
(39) Laforgue, A.; Simon, P.; Sarrazin, C.; Fauvarque, J.-F. *J. Power Sources* **1999**, *80*, 142−148.
(40) Chen, J. H.; Huang, Z. P.; Wang, D. Z.; Yang, S. X.; Li, W. Z.; Wen, J. G.; Ren, Z. F. *Synth. Met.* **2002**, *125*, 289−294.
(41) Frackowiak, E.; Khomenko, V.; Jurewicz, K.; Lota, K.; Béguin, F. *J. Power Sources* **2006**, *153*, 413−418.
(42) Khomenko, V.; Frackowiak, E.; Béguin, F. *Electrochim. Acta* **2005**, *50*, 2499−2506.
(43) Hughes, M.; Chen, G. Z.; Shaffer, M. S. P.; Fray, D. J.; Windle, A. H. *Chem. Mater.* **2002**, *14*, 1610−1613.
(44) An, K. H.; Jeon, K. K.; Heo, J. K.; Lim, S. C.; Bae, D. J.; Lee, Y. H. *J. Electrochem. Soc.* **2002**, *149*, A1058−A1062.
(45) Lota, K.; Khomenko, V.; Frackowiak, E. *J. Phys. Chem. Solids* **2004**, *65*, 295−301.
(46) Maser, W. K.; Benito, A. M.; Callejas, M. A.; Seeger, T.; Martínez, M. T.; Schreiber, J.; Muszynski, J.; Chauvet, O.; Osváth, Z.; Koós, A. A.; Biró, L. P. *Mater. Sci. Eng., C* **2003**, *23*, 87−91.
(47) Xiao, Q.; Zhou, X. *Electrochim. Acta* **2003**, *48*, 575−580.
(48) Zhou, C.; Kumar, S.; Doyle, C. D.; Tour, J. M. *Chem. Mater.* **2005**, *17*, 1997−2002.
(49) Chen, G. Z.; Shaffer, M. S. P.; Coleby, D.; Dixon, G.; Zhou, W.; Fray, D. J.; Windle, A. H. *Adv. Mater.* **2000**, *12*, 522−526.
(50) Hughes, M.; Shaffer, M. S. P.; Renouf, A. C.; Singh, C.; Chen, C. Z.; Fray, D. J.; Windle, A. H. *Adv. Mater.* **2002**, *14*, 382−385.
(51) Kim, J.-Y.; Kim, K. H.; Kim, K. B. *J. Power Sources* **2008**, *176*, 396−402.
(52) Peng, C.; Jin, J.; Chen, G. Z. *Electrochim. Acta* **2007**, *53*, 525−537.
(53) Kang, Y. K.; Lee, O.-S.; Deria, P.; Kim, S. H.; Park, T.-H.; Bonnell, D. A.; Saven, J. G.; Therien, M. J. *Nano Lett.* **2009**, *9*, 1414−1418.
(54) Deria, P.; Sinks, L. E.; Park, T.-H.; Tomezsko, D. M.; Brukman, M. J.; Bonnell, D. A.; Therien, M. J. *Nano Lett.* **2010**, *10*, 4192−4199.
(55) Dietrich, M.; Heinze, J.; Heywang, G.; Jonas, F. *J. Electroanal. Chem.* **1994**, *369*, 87−92.
(56) Kumar, A.; Welsh, D. M.; Morvant, M. C.; Piroux, F.; Abboud, K. A.; Reynolds, J. R. *Chem. Mater.* **1998**, *10*, 896−902.
(57) Stenger-Smith, J. D.; Guenthner, A.; Cash, J.; Irvin, J. A.; Irvin, D. J. *J. Electrochem. Soc.* **2010**, *157*, A298−A304.
(58) McEwen, A. B.; Ngo, H. L.; LeCompte, K.; Goldman, J. L. *J. Electrochem. Soc.* **1999**, *146*, 1687−1695.
(59) Asavapiriyanont, S.; Chandler, G. K.; Gunawardena, G. A.; Pletcher, D. *J. Electroanal. Chem.* **1984**, *177*, 229−244.
(60) Downard, A. J.; Pletcher, D. *J. Electroanal. Chem.* **1986**, *206*, 147−152.
(61) Upon device disassembly, charge storage media based on the pure polymer showed evident surface degradation (e.g., scratches, pinholes, peeling) following evaluation periods lasting up to 4 days; in contrast, hybrid composite-based devices manifest charge storage media that appeared pristine following 4 days of continued redox cycling.
(62) (a) Burke, A. J. *Power Sources* **2000**, *91*, 37−50. (b) Stenger-Smith, J. D.; Irvin, J. A. personal communication, 2007.
(63) Stoller, M. D.; Ruoff, R. S. *Energy Environ. Sci.* **2010**, *3*, 1294−1301.
(64) Rosario-Canales, M. R.; Deria, P.; Kang, Y.; Therien, M.; Santiago-Aviles, J. *ECS Trans.* **2008**, *16*, 93−101.